--- Supporting Information for ---

^{17}O NMR Investigation of Water Structure and Dynamics

Eric G. Keeler, Vladimir K. Michaelis[†] and Robert G. Griffin*

Department of Chemistry and Francis Bitter Magnet Laboratory, Massachusetts Institute

of Technology, Cambridge, Massachusetts, 02139 USA

Corresponding Author

*Robert G. Griffin, rgg@mit.edu

[†]Current Address: Department of Chemistry, University of Alberta, Edmonton, Alberta,

T6G 2G2 Canada

Terminology and Definitions

NMR spectra of half-integer nuclear spin quadrupolar nuclei can be used to determine the local structure around the quadrupolar nucleus of interest via chemical shift and quadrupolar information. ^{17}O MAS NMR spectra typically show a central transition (1/2 ↔ -1/2) peak subject to the second-order quadrupolar interaction that can be described by the quadrupolar coupling constant, C_Q, and the asymmetry parameter, η_Q.

$$C_Q = \frac{eV_{zz}Q}{h}$$

(1)

$$\eta_Q = \frac{\left(V_{xx} - V_{yy}\right)}{V_{zz}}$$

(2)

Here e is the charge of an electron, Q is the quadrupolar moment intrinsic to the nucleus of interest, h is the Planck constant, and V_{nn} are eigenvalues of the electric field gradient (EFG) tensor, with V_{zz} being the largest component ($|V_{zz}| \geq |V_{yy}| \geq |V_{xx}|$).[1-4]

Chemical shift anisotropy (CSA) can influence the NMR spectra of quadrupolar nuclei, such as ^{17}O. To assist in isolating the effects of the chemical shift tensor on the spectra experiments are performed at multiple magnetic fields. The increase in contribution due to CSA combined with the subsequent decrease in the effect of the quadrupolar interaction allows for less ambiguous determinations of the interaction tensors as the external magnetic field is increased. The discussion that follows will employ the IUPAC definitions for chemical shift interactions.[5] The isotropic chemical shift is defined as the trace of the chemical shift tensor,

$$\delta_{iso} = \frac{1}{3}(\delta_{zz} + \delta_{yy} + \delta_{xx}) \tag{3}$$

where, δ_{zz}, δ_{yy} and δ_{xx} are the principal components of the second rank chemical shift tensor. The chemical shift tensor can be further described by the chemical shift anisotropy, ζ_δ and asymmetry parameter, η_δ,

$$\zeta_\delta = \delta_{zz} - \delta_{iso} \tag{4}$$

$$\eta_\delta = \frac{\delta_{yy} - \delta_{xx}}{\zeta_\delta} \tag{5}$$

when adopting the Haeberlen convention[5-7], where

$$\left|\delta_{zz}\right| \geq \left|\delta_{yy}\right| \geq \left|\delta_{xx}\right| \tag{6}$$

Quantum chemical calculations determine the nuclear shielding tensor rather than the chemical shift tensor,

$$\delta_{nn} = \sigma_{nn} - \sigma_{ref} \tag{7}$$

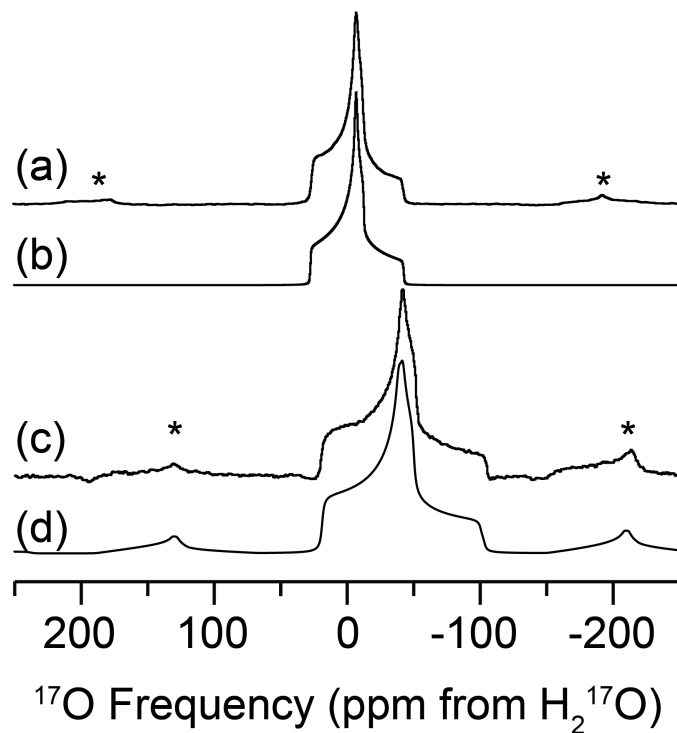The dipolar coupling tensor will be describe herein using the dipolar coupling constant, D.

Figure S1. ^{17}O MAS NMR spectra and simulation of $Ba(ClO_3)_2 \cdot H_2O$ at (a,b) 18.8 T ($\omega_{0H}/2\pi = 800$ MHz) and (c,d) 14.1 T ($\omega_{0H}/2\pi = 600$ MHz) at room temperature. Simulated NMR parameters: $C_Q = 6.9 \pm 0.2$ MHz, $\eta_Q = 0.98 \pm 0.05$, $\delta_{iso} = 21 \pm 1$ ppm. Asterisks (*) denote spinning sidebands.
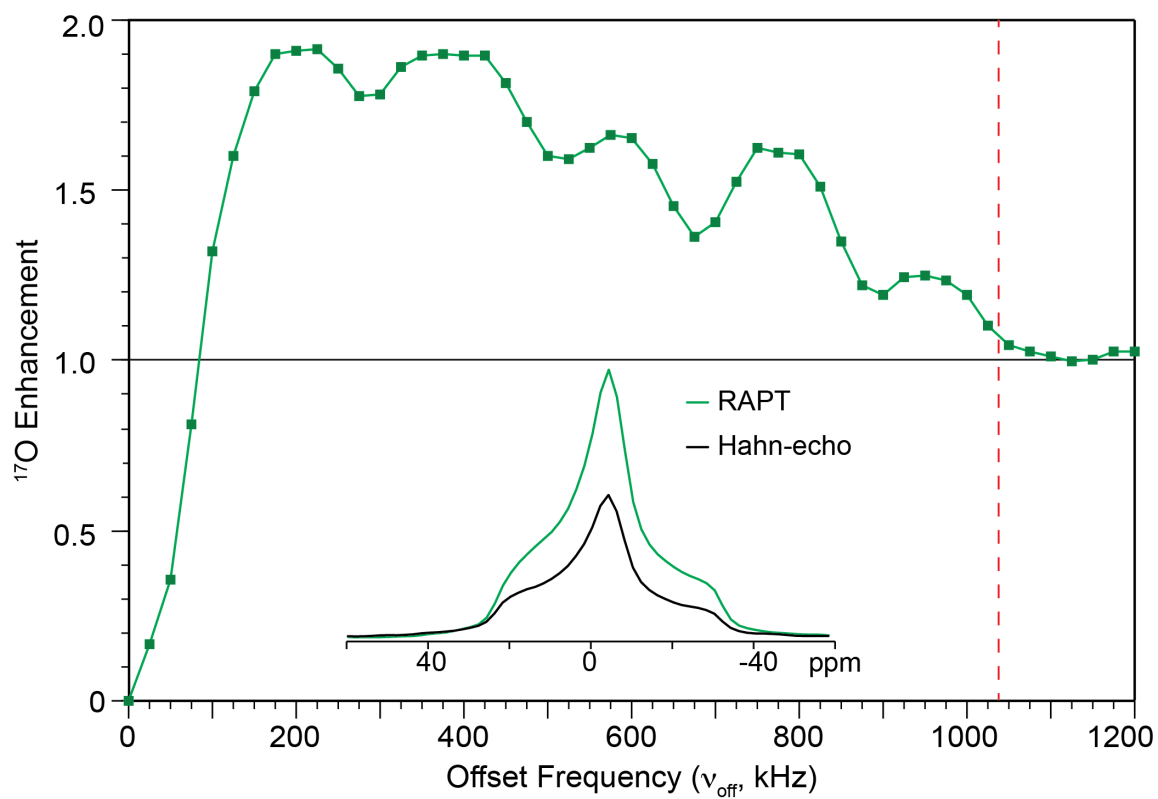
Figure S2. RAPT profile of $Ba(ClO_3)_2 \cdot H_2{}^{17}O$. The edge frequency ($\nu_{edge}$) is indicated by the dotted vertical line (red) and is related to the quadrupole coupling constant by the equation: $\nu_{edge} = 3C_Q/(2I(2I-1))$. Inset: RAPT enhancement with $\nu_{off} = 350$ kHz.
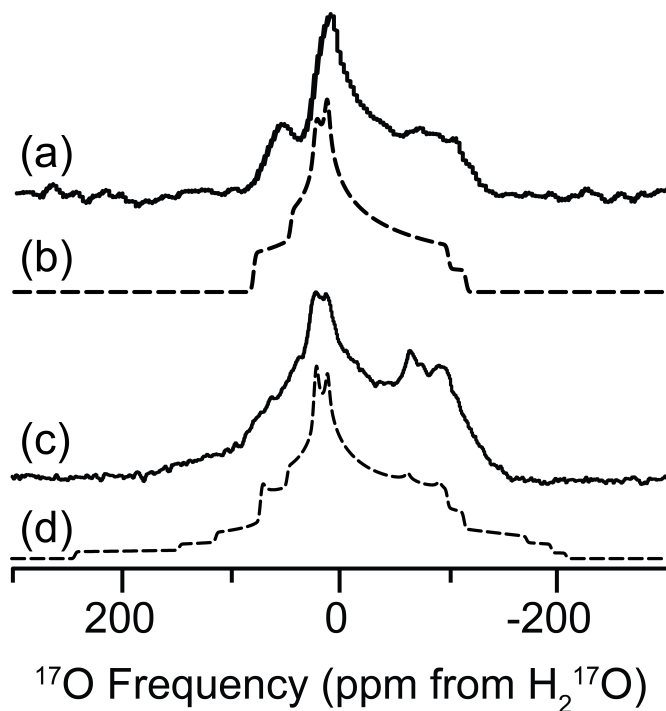
Figure S3: Stationary ^{17}O NMR spectra and simulation of $Ba(ClO_3)_2 \bullet H_2O$ at 21.1 T ($\omega_{0H}/2\pi$ = 900 MHz) and 270 K with (a,b) and without (c,d) continuous-wave ^1H decoupling ($\gamma B_1/2\pi$ = 100 kHz). Simulated NMR parameters: (b) C_Q = 6.9 ± 0.2 MHz, η_Q = 0.98 ± 0.02, δ_{iso} = 21 ± 1 ppm, ζ_δ = 25 ± 5 ppm, and η_δ = 0.25 ± 0.25; (c) identical to (b) with the addition of D_{O-H} = 10 ± 2 kHz (η=1).

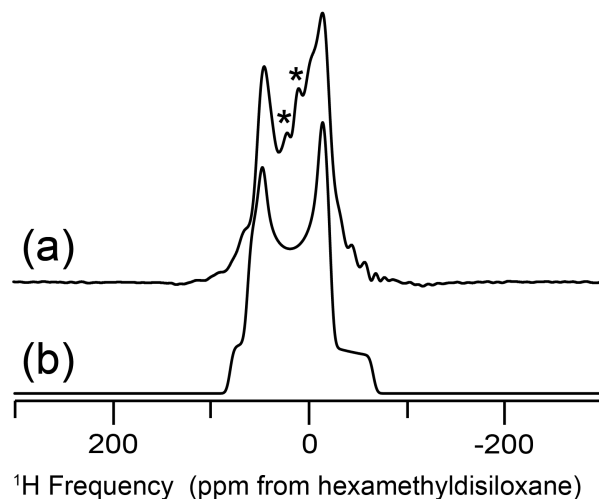**Figure S4.** Stationary ^1H NMR (a) spectra and (b) simulation of $Ba(ClO_3)_2 \cdot H_2O$ at 16.4 T ($\omega_{0H}/2\pi$ = 699 MHz) Simulations with CSA parameters: δ_{iso} = 4 ± 1 ppm, ζ_δ = -10 ± 2 ppm, η_δ= 0.9 ± 0.2, and dipole coupling constant, D = 29 ± 1 kHz. Peaks indicated with asterisks (*) are from the rotor and stator background. Simulation is a verification of Carnevale et al.[15]
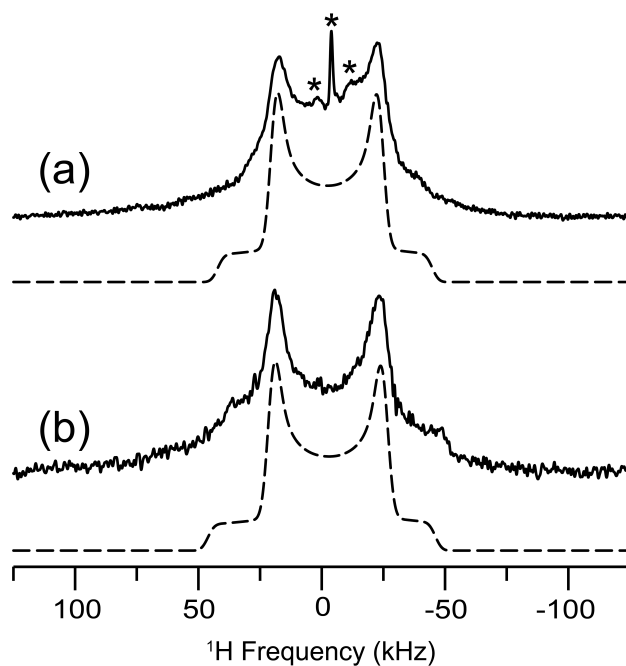
Figure S5. Stationary ^{1}H NMR spectra and simulations of $Ba(ClO_3)_2 \cdot H_2O$ at 5 T ($\omega_{0H}/2\pi = 212.026$ MHz) at (a) 300 K and (b) 95 K. (a) Simulation (dashed) using with CSA parameters: $\zeta_\delta = -10 \pm 2$ ppm, $\eta_\delta = 0.9 \pm 0.2$, and dipole coupling constant, $D = 29 \pm 1$ kHz. (b) Simulation (dashed) using with CSA parameters: $\zeta_\delta = -18 \pm 2$ ppm, $\eta_\delta = 0.2 \pm 0.2$, and dipole coupling constant, $D = 31 \pm 1$ kHz. Peaks indicated with asterisks (*) are from the probe background.
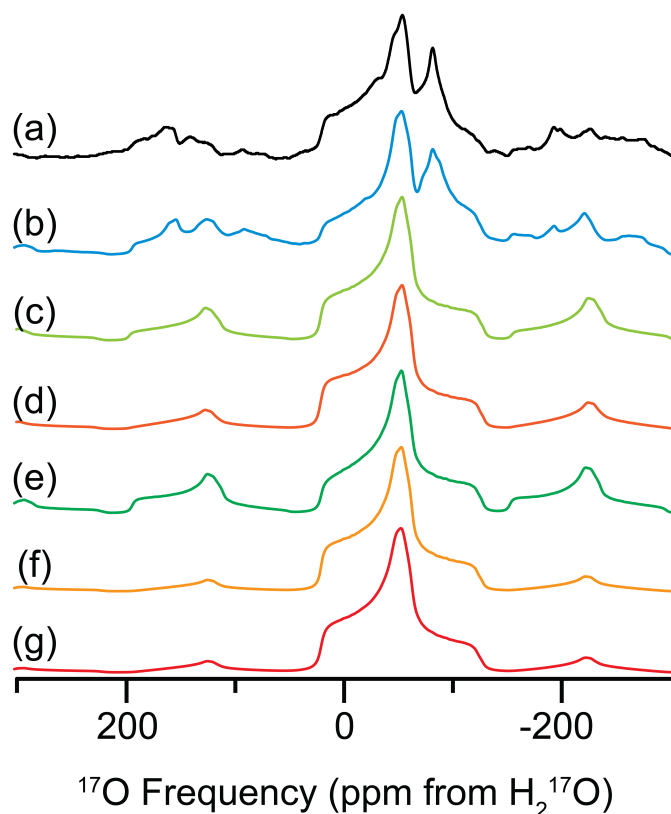
Figure S6. Experimental (a) and simulated (b-g) ^{17}O MAS spectra of $Ba(ClO_3)_2 \cdot H_2{}^{17}O$ at 14.1 T ($\omega_{0H}/2\pi$ = 600 MHz): (a) experimental spectrum of $Ba(ClO_3)_2 \cdot H_2{}^{17}O$ at 105 ± 5 K without ^1H decoupling, (b) simulation of $Ba(ClO_3)_2 \cdot H_2{}^{17}O$ in the rigid lattice limit, (c) simulation of MAS NMR spectrum of $Ba(ClO_3)_2 \cdot HD^{17}O$ in the rigid lattice limit, (d) simulation of $Ba(ClO_3)_2 \cdot D_2{}^{17}O$ in the rigid lattice limit, (e) simulation of $Ba(ClO_3)_2 \cdot H_2{}^{17}O$ in the rigid lattice limit excluding the ^1H-^1H dipole coupling; (f) simulation of $Ba(ClO_3)_2 \cdot H_2{}^{17}O$ in the rigid lattice limit excluding the ^{17}O -^1H dipole coupling; (g) simulation of ^{17}O in the rigid lattice limit with 100 kHz ^1H decoupling.

Figure S7. Plots of the refined structure calculations using GIPAW that relate the O-H distance to (a) calculated C_Q and (b) calculated η_Q. The black, red, and green filled points are grouped as the minimum, average, and maximum HOH angle, respectively according to Chiari *et al.*[16] The open blue points represent NMR refined structures with fixed H—H distance of 1.62 ± 0.02 Å; the open blue circle/square represents

the best fit NMR refined structure that is near to the thermally corrected O-H distance.[17] The dashed vertical line (grey) represents the O-H distance from the H-optimized GIPAW calculation.
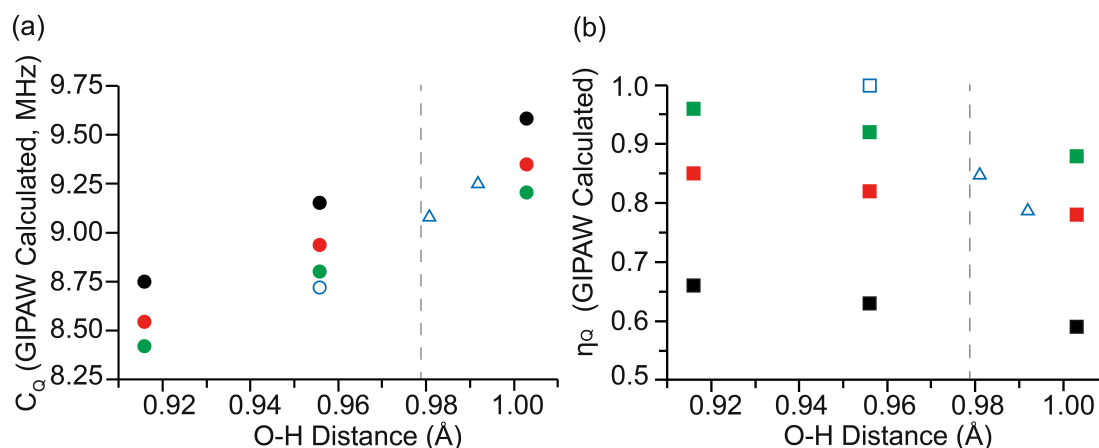
(a)

(b)

Figure S8. Plots of the refined structure calculations using GIPAW that relate the ∠HOH angle to (a) calculated C_Q and (b) calculated η_Q. The black, red, and green filled points are grouped as the minimum, average, and maximum O-H distance respectively according to Chiari *et al.*[16] The open blue points represent NMR refined structures with fixed H---H distance of 1.62 ± 0.02 Å; the open blue circle/square represent the best fit NMR refined structure that is near to the thermally corrected O-H distance.[17] The dashed vertical line represents the ∠HOH angle from the H-optimized GIPAW calculation.
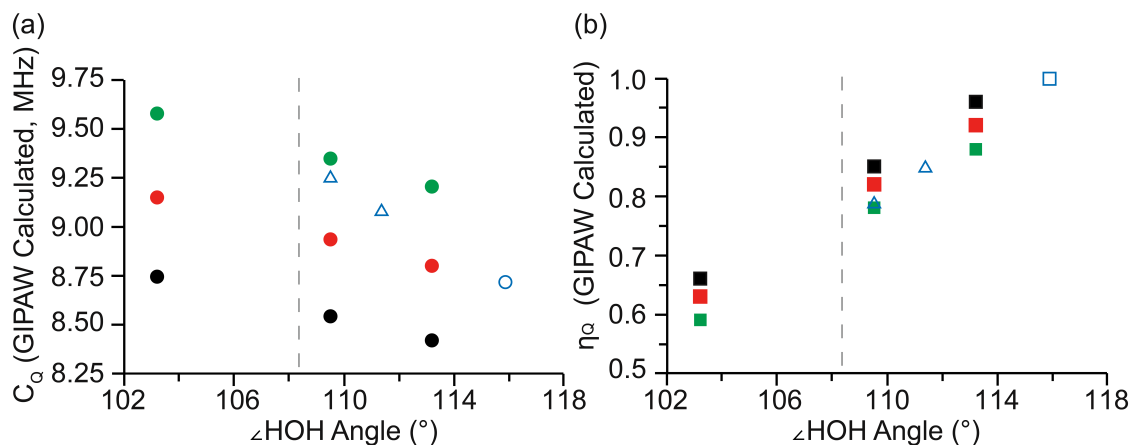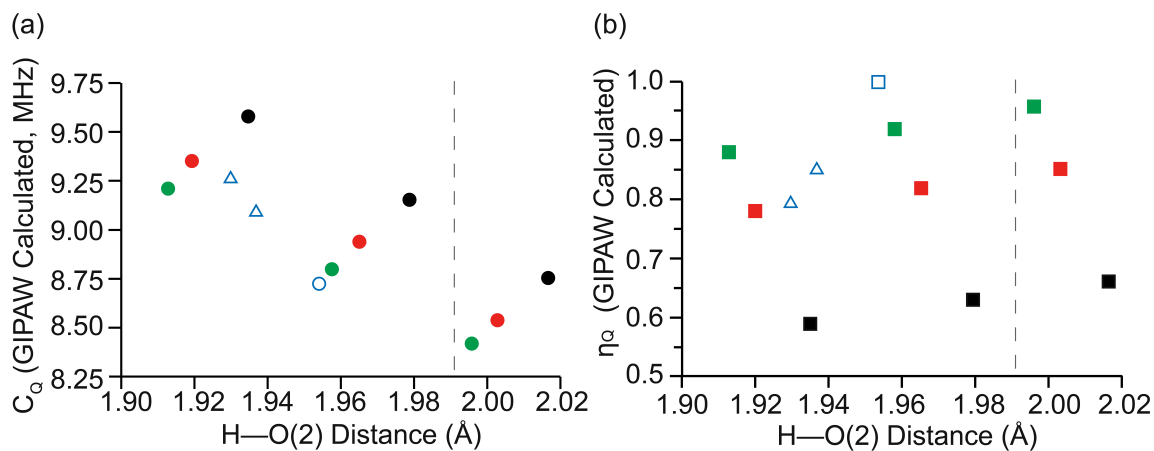
Figure S9. Plots of the refined structure calculations using GIPAW that relate the H—O(2) distance to (a) calculated C_Q and (b) calculated η_Q. The black, red, and green filled points are grouped as the minimum, average, and maximum ∡HOH angle respectively according to Chiari *et al.*[16] The open blue points represent NMR refined structures with fixed H---H distance of 1.62 ± 0.02 Å; the open blue circle/square represents the best fit NMR refined structure that is near to the thermally corrected O-H distance.[17] The dashed vertical line (grey) represents the H—O(2) distance from the H-optimized GIPAW calculation.

Table S1: Structural details and GIPAW calculated ^{17}O EFG parameters for $Ba(ClO_3)_2 \cdot H_2O$

Structure	O-H distance (Å)	∠ HOH angle (°)	H---H distance (Å)	H—O(2) distance (Å)	C_Q (MHz)	η_Q
H-opt neutron structure	0.979	108.4	1.588	1.991	9.163	0.76
1	0.916	103.2	1.436	2.017	8.747	0.66
2	0.916	109.5	1.496	2.003	8.545	0.85
3	0.916	113.2	1.529	1.996	8.421	0.96
4	0.956	103.2	1.498	1.979	9.151	0.63
5	0.956	109.5	1.561	1.965	8.936	0.82
6	0.956	113.2	1.596	1.958	8.802	0.92
7	1.003	103.2	1.572	1.935	9.58	0.59
8	1.003	109.5	1.638	1.920	9.348	0.78
9	1.003	113.2	1.675	1.913	9.205	0.88
10	0.992	109.5	1.620	1.930	9.256	0.79
11	0.956	115.9	1.620	1.954	-8.718	1.00
12	0.918	111.4	1.620	1.937	9.089	0.85

Table S2: GIPAW calculated ^{17}O EFG parameters for $Ba(ClO_3)_2 \cdot H_2O$

	C_Q (MHz)	η_Q	σ_{iso} (ppm)	ζ_δ (ppm)	η_δ	σ_{11} (ppm)	σ_{22} (ppm)	σ_{33} (ppm)
H-opt	9.163	0.76	254.99	20.307	0.230	267.479	262.808	234.683

References

1.   Ashbrook, S. E.; Wimperis, S., Quadrupolar Coupling: An Introduction and Crystallographic Aspects. e*MagRes*, John Wiley & Sons, Ltd: 2007.

2.   Man, P. P., *Encyclopedia of Analytical Chemistry*. John Wiley and Sons: Chichester, 2000; p 12224-12265.

3.   Slichter, C. P., *Principles of Magnetic Resonance, with Examples from Solid State Physics*. Harper & Row: New York,, 1963; p 246 p.

4.   Taulelle, F., *NMR of Quadrupolar Nuclei in the Solid State*. Kluwer Academic Publishers: London, 1988; Vol. 322, p 476.

5.   Harris, R. K.; Becker, E. D.; De Menezes, S. M. C.; Granger, P.; Hoffman, R. E.; Zilm, K. W., Further Conventions for NMR Shielding and Chemical Shifts (Iupac Recommendations 2008). *Pure and Applied Chemistry* **2008,** *80*, 59-84.

6.   Haeberlen, U., *High Resolution NMR in Solids : Selective Averaging*. Academic Press: New York, 1976.

7.   Mehring, M., *Principles of High-Resolution NMR in Solids*. 2nd, rev. and enl. ed.; Springer-Verlag: Berlin ; New York, 1983; p viii, 342 p.

8.   Yao, Z.; Kwak, H. T.; Sakellariou, D.; Emsley, L.; Grandinetti, P. J., Sensitivity Enhancement of the Central Transition NMR Signal of Quadrupolar Nuclei under Magic-Angle Spinning. *Chemical Physics Letters* **2000,** *327*, 85-90.

9.   Prasad, S.; Kwak, H. T.; Clark, T.; Grandinetti, P. J., A Simple Technique for Determining Nuclear Quadrupole Coupling Constants with RAPT Solid-State NMR Spectroscopy. *Journal of the American Chemical Society* **2002,** *124*, 4964-4965.

10.   Michaelis, V. K.; Keeler, E. G.; Ong, T.-C.; Craigen, K. N.; Penzel, S. A.; Wren, J. E. C.; Kroeker, S.; Griffin, R. G., Structural Insights into Bound Water in Crystalline Amino Acids: Experimental and Theoretical ^{17}O NMR. *The Journal of Physical Chemistry B* **2015,** *119*, 8024-8036.

11.   Eichele, K. *WSolids1 NMR Simulation Package*, 1.20.21; 2013.

12.   Massiot, D.; Fayon, F.; Capron, M.; King, I.; Le Calve, S.; Alonso, B.; Durand, J. O.; Bujoli, B.; Gan, Z. H.; Hoatson, G., Modelling One- and Two-Dimensional Solid-State NMR Spectra. *Magnetic Resonance in Chemistry* **2002,** *40*, 70-76.

13.   Bak, M.; Rasmussen, J. T.; Nielsen, N. C., Simpson: A General Simulation Program for Solid-State NMR Spectroscopy. *Journal of Magnetic Resonance* **2000,** *147*, 296-330.

14.   Adiga, S.; Aebi, D.; Bryce, D. L., EFG Shield - a Program for Parsing and Summarizing the Results of Electric Field Gradient and Nuclear Magnetic Shielding Tensor Calculations. *Canadian Journal of Chemistry,* **2007,** *85*, 496-505.

15.   Carnevale, D.; Ashbrook, S. E.; Bodenhausen, G., Solid-State NMR Measurements and DFT Calculations of the Magnetic Shielding Tensors of Protons of Water Trapped in Barium Chlorate Monohydrate. *RSC Advances* **2014,** *4*, 56248-56258.

16.   Chiari, G.; Ferraris, G., The Water Molecule in Crsytalline Hydrates Studied by Neutron Diffraction. *Acta Crystallographica* **1982,** *B 38*, 2331-2341.

17.   Sikka, S. K.; Momin, S. N.; Rajagopa.H; Chidamba.R, Neutron-Diffraction Refinement of Crystal Structure of Barium Chlorate Monohydrate $Ba(ClO_3)_2 \cdot H_2O$. *Journal of Chemical Physics* **1968,** *48*, 1883-1890.